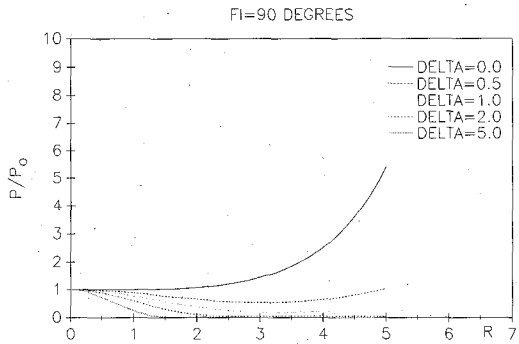

Fig. 4. Power focusing relative to power at the center versus R for ϕ = 90 degrees.

comes focused near the center of the cylinder. At low frequency (i.e., Δ is small where displacement current is negligible) there is no focusing.

IV. Concluding Remarks

While the present model is highly idealized, it does show that, with a cos ϕ excitation, the power can be focused on the axis of the cylinder. To deal with a cylinder of finite length and an actual wire loop, a three-dimensional analysis is required, but we can assert that in the principal plane of the loop, the result should be qualitatively similar to the two-dimensional model. Of course, for a practical scheme, we would limit the cylinder radius a to reduce the peripheral heating.

References

[1] F. K. Storm, R. S. Elliott, W. H. Harrison, and D. L Morton, "Clinical RF hyperthermia by magnetic loop induction: A new approach to human cancer therapy," *IEEE Trans. Microwave Theory Tech.*, vol. 30, no. 8, pp. 1149–1157, Aug. 1982.

[2] J. C. Lin, Ed., Special Issue on Phased Arrays, *IEEE Trans Microwave Theory Tech.*, vol. 34, no. 5, pp. 481–648, May 1986.

[3] J. R. Wait and M. Lumori, "Focused heating in cylindrical targets," Pt. II., *IEEE Trans.*, vol. 34, no. 3, pp. 357–359, Mar. 1986.

[4] C. M. Rappaport, "Synthesis of optimum microwave antenna applications for use in treating deep localized tumors," in *Progress in Electromagnetic Research*. Amsterdam: Elsevier, vol. 1, no. 2, 1989, pp. 175–240.

Bias-Dependence of the Intrinsic Element Values of InGaAs/InAlAs/InP Inverted Heterojunction Bipolar Transistor

Bahman Meskoob, Sheila Prasad, Mankuan Vai, James C. Vlcek, Hiroya Sato, and Clifton G. Fonstad

***Abstract*—The small-signal S parameters of an inverted InGaAs/InAlAs/InP heterojunction bipolar transistor are measured at 39 bias points covering the entire useful bias region. Small-signal model fitting is performed at each bias point. The results of the small-signal model fitting show that in this device it is sufficient to take five intrinsic elements of the model to be bias dependent. The methodology and the results of the simulations are presented here.**

Manuscript received July 30, 1991; revised November 15, 1991. This work was supported in part by NSF grant ECS-9005837 to Northeastern University.

B. Meskoob, S. Prasad, M-K. Vai are with the Department of Electrical and Computer Engineering, Northeastern University, Boston, MA, 02115.

C. F. Fonstad is and J. C. Vlcek was with the Department of Electrical Engineering and Computer Science and Center for Materials Science and Engineering, Massachusetts Institute of Technology, Cambridge, MA 02139. J. C. Vlcek is now with Epi Corporation, St. Paul, MN 55101.

H. Sato is with the Sharp Corporation, Nara 632, Japan.

IEEE Log Number 9107023.

I. Introduction

The heterojunction bipolar transistor (HBT) is rapidly emerging as a significant device for applications at microwave frequencies. Kim *et al.* [1] have reviewed the GaAs device and IC technology in detail. There has also been a rapid development of the InP/In(Al, Ga)As HBT technology [2] and the inverted HBT structure is being explored [3]. A small signal equivalent circuit model has been developed [4] for this structure. However, for many microwave applications, it is also necessary to have a large-signal model.

For large signal device modeling, the voltage and/or current dependence of the model elements is required. The dynamic variation of the element values has usually been assumed to be the same as the static (or bias) variation. This assumption has been proved to work quite well for many design applications. The popularity of this *quasi-static* assumption is due to the simplicity of small signal measurements and the subsequent modeling of transistors.

As a first step towards the large signal modeling, we have investigated the bias dependence of five intrinsic elements of the small signal model of the inverted HBT having the layer structure shown in Fig. 1. This has been done through small-signal S parameter measurements and model fitting using the commercial software Touchstone [5]. The results are presented in this paper.

II. Procedure

Fig. 2 shows the HBT's I-V characteristics. Small-signal S parameters were measured on wafer from 0.05 to 40 GHz at 39 different bias points. These were chosen along constant base current (I_b) curves at different V_{ce} values. Since this device has an f_T of 23 GHz, measurements above 26 GHz were not used for modeling. To reduce the computation time, only 16 frequencies were chosen. These are 0.05, 0.1, 0.2, 0.4, 0.8, 1.6 GHz; 3 to 11 GHz in 2 GHz increments and 11 to 26 GHz in 3 GHz increments.

The small signal equivalent circuit is shown in Fig. 3. Initially this model was fitted to measurements at the bias point of I_b = 150 μA, V_{ce} = 1.6 V. Due to the large number of parameters (element values) in the optimization process, it is difficult to judge the physical validity of the optimized parameters. In order to test the validity of the element values, a fit at zero bias (I_b = 0 μA, V_{ce} = 0 V) was performed. Since at zero bias the device is passive (α_o = 0) and both R_e and R_o (= $1/g_o$) are very large, three of the five bias-dependent elements are effectively removed. Therefore, a variation of only two bias-dependent elements (namely, C_e and C_c) should result in a good fit at zero bias. The fit at (150 μA, 1.6 V) was modified until the zero bias fit was also acceptable. Fig. 4 shows the normalized deviation defined by

$$\text{Normalized Deviation} = \frac{1}{39}\sum_{\text{Bias}}\left|\frac{M-S}{M}\right|$$

where M is the measured and S is the simulated vector S parameter and the number of bias points used is 39. The deviation is typically within 10% except for S_{12} at low frequencies. Due to the small magnitude of S_{12} at low frequencies, any error in its measured magnitude or phase results in a significant error in the calculation of the normalized deviation.

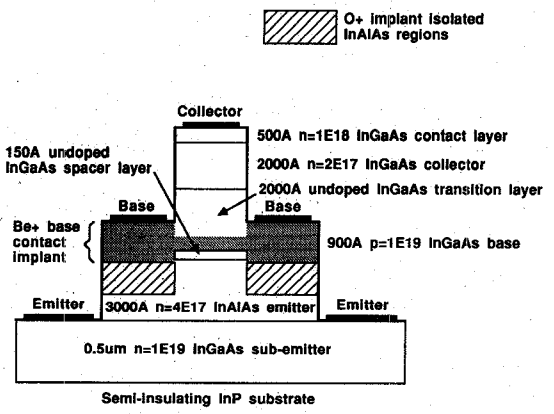

Fig. 1. Vertical structure of the 5 × 10 μm non-self-aligned InAlAs/InGaAs inverted HBT (not to scale).

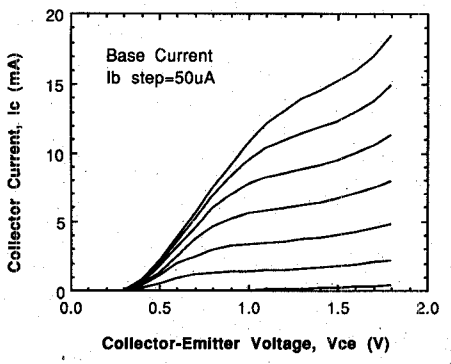

Fig. 2. Collector current (I_c) versus collector-emitter voltage (V_{ce}) transfer characteristics of the HBT, with 50 μA base current steps.

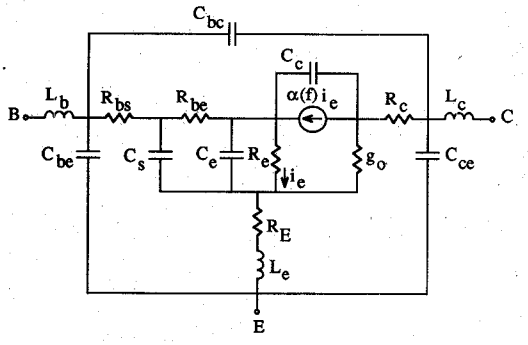

$$\alpha(\omega) = \alpha_0 \frac{\sin(\omega\tau_c/2)}{\omega\tau_c/2} \frac{e^{-j\omega(\tau_c/2 + m\tau_b)}}{1 + j\omega\tau_b}, \quad m = 0.22$$

Fig. 3. Equivalent circuit model of the inverted HBT.

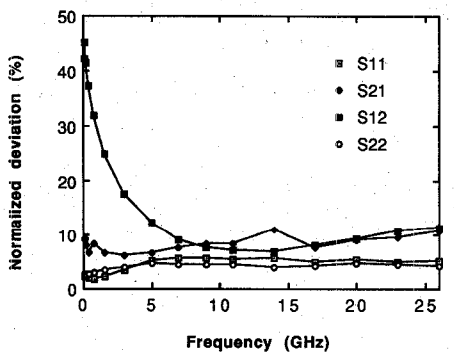

Fig. 4. Normalized deviation of the S parameter fit averaged over 39 different bias points.

TABLE I
FIXED ELEMENT VALUES OF THE MODEL IN UNITS Ω fF, pH, ps

$R_{bs} + R_{be}$	165	L_b	30
C_s	*	L_c	49
R_e	17	L_e	10
R_E	32	C_{be}	40
τ_c	1.42	C_{ce}	31
τ_b	0.72	C_{bc}	6.3

*Explanation in text.

The parasitic elements, C_{bc}, C_{bc}, C_{ce}, L_b, L_e, L_c, contact resistors, R_{bs}, R_c, R_E, and the intrinsic base resistor, R_{be}, were assumed to be linear and invariant with bias. The base and collector transit times, τ_b and τ_c, were also assumed to be constants. Due to the heavy doping of the base, the basewidth and therefore the base transit time does not change with bias. The existence of the base-collector undoped transition layer makes the depletion width and therefore τ_c insensitive to bias. To a first approximation, the total depletion width of this junction is $w = (w_t^2 + w_o^2)^{1/2}$, where w_t is the transition layer width and w_o is the depletion width of the same junction without the transition layer. For the device considered here, the maximum change in total depletion width is less than 20% for relevant values of V_{cb}. Table I shows the fixed element values. As a practical matter, it is found that since R_{be} is much smaller than R_{bs}, it is impossible to separate C_s (the extrinsic base-emitter depletion capacitance) from C_e, and R_{be} from R_{bs} in any meaningful way. Thus in Table I we list $R_{be} + R_{bs}$, rather than the individual values of R_{be} and R_{bs}. Furthermore in the discussion below of the bias dependence of C_e, it should be kept in mind that the results actually represent ($C_s + C_e$) rather than C_e alone even though C_s is not bias dependent.

The five bias-dependent intrinsic elements are R_e, C_e, C_c, α_o, and g_o. Considering α_o and g_o, the low frequency S_{21} and S_{22} values (being insensitive to reactive elements and most sensitive to α_o and g_o) were used for the manual tuning of these two elements. The bias variations of α_o and g_o as calculated from the I-V characteristics (Fig. 2) were taken as a starting point during this manual tuning. α_o and g_o were then fixed during optimizations. The three parameters R_e, C_e and C_c were subsequently optimized.

III. RESULTS

The results of the simulations are shown in Figs. 5–9. As expected, the variation of α_o and g_o agrees with the I-V characteristics. g_o increases as the bias approaches the saturation region, and for large V_{ce} and I_b values when avalanching occurs. α_o decreases as bias approaches the saturation region and initially increases with increasing collector current before its value saturates. Fig. 7 shows that R_e has a strong inverse dependence on I_b. Fig. 8 shows that C_e starts at 0.12 pF and increases monotonically with increasing I_b. The dependence of both R_e and C_e on I_b agrees with the simple homojunction case where $R_e = kT/qI_b$ and $C_e = C_{je} + \tau qI_b/kT$ where C_{je} is the base-emitter depletion capacitance. Figs. 7 and 8 also show that R_e and C_e are relatively insensitive to V_{ce}. At the base current of 150 μA, Fig. 8 shows a large variation in C_e with respect to V_{ce}. This variation could be due to the numerical optimization routine rather than physical phenomena. Fig. 9 shows that C_c varies with both V_{ce} and I_b. The inverse dependence of C_c on V_{ce} fits the simple pn-junction theory in that as V_{ce} increases, V_{cb} also increases, and therefore C_c decreases. Fig. 9 also shows that, as the bias approaches the saturation region of the I-V characteristics, the dependence of C_c on I_b becomes significant. Close to

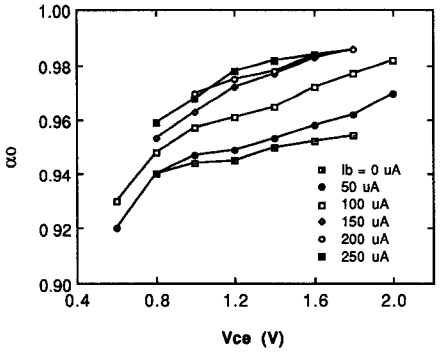

Fig. 5. Plot of the current-transfer ratio (α_o) with variation in the dc bias.

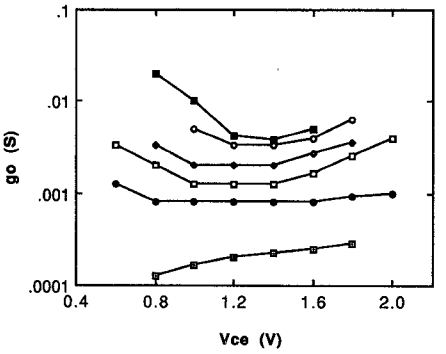

Fig. 6. Plot of the output conductance (g_o) with variation in the dc bias.

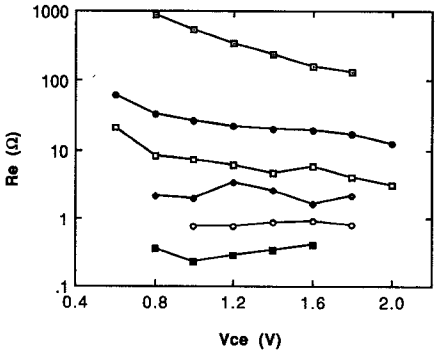

Fig. 7. Plot of the dynamic emitter resistance (R_e) with variation in the dc bias.

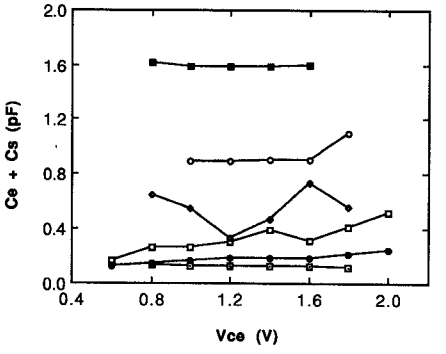

Fig. 8. Plot of the emitter-base diffusion and depletion capacitance (C_e + C_s) with variation in the dc bias.

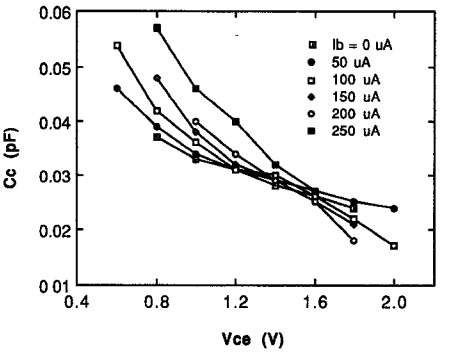

Fig. 9. Plot of the collector-base junction capacitance (C_c) with variation in the dc bias.

saturation, as I_b increases, V_{cb} decreases and since V_{cb} is small, the increase in junction capacitance is significant.

IV. Conclusion

A small signal model has been fitted to S parameter measurements of an inverted InGaAs/InAlAs/InP heterojunction bipolar transistor. The fit was determined over a set of bias values covering the entire useful range of the I-V characteristics. As a result of this measurement and modeling effort, it is clear that consideration of the bias variation of only five intrinsic elements is sufficient to obtain a model valid over a large bias range. Further work on the contribution of each bias dependent element to the overall intermodulation distortion and harmonic distortion is in progress.

References

[1] M. E. Kim, A. K. Oki, G. M. Gorman, D. K. Umemoto, and J. B. Camou, "GaAs heterojunction bipolar transistor device and IC technology for high performance analog and microwave applications," *IEEE Trans. Microwave Theory Tech.*, vol. 37, pp. 1286–1303, Sept. 1989.

[2] Y. K. Chen, R. N. Nottenburg, M. B. Panish, R. A. Hamm, and D. A. Humphrey, "Subpicosecond InP/InGaAs heterojunction bipolar transistors," *IEEE Electron Device Lett.*, vol. 10, pp. 267–269, June 1989.

[3] H. Sato, J. C. Vlcek, C. G. Fonstad, B. Meskoob, and S. Prasad, "InGaAs/InAlAs/InP Collector-up microwave heterojunction bipolar transistors," *IEEE Electron Device Lett.*, vol. 11, pp. 457–459, Oct. 1990.

[4] B. Meskoob, S. Prasad, M-K. Vai, J. C. Vlcek, H. Sato, C. G. Fonstad, and C. Bulutay, "Small signal equivalent circuit model for the collector-up InGaAs/InAlAs/InP heterojunction bipolar transistor," submitted for publication.

[5] "Touchstone, Version 2.1," EEsof, Inc., 1990.

On the Representational Nonuniqueness of Uniform Waveguide Eigenvalue Formulas

P. L. Overfelt

***Abstract*—In the following, we find that for uniform perfectly conducting waveguides characterized by rectilinear boundaries and exact eigenvalue formulas, such formulas are not representationally unique.**

Manuscript received May 14, 1991; revised December 30, 1991.

The author is with the Naval Air Warfare Center Weapons Division, Research Department, Code 3814, China Lake, CA 93555.

IEEE Log Number 9106762.